Pore-Width-Dependent Ordering of C_2H_5OH Molecules Confined in Graphitic Slit Nanospaces

T. Ohkubo,[†] T. Iiyama,[†] K. Nishikawa,[‡] T. Suzuki,[†] and K. Kaneko*,[†]

Physical Chemistry, Material Science, Graduate School of Natural Science and Technology, Chiba University, 1-33 Yayoi, Inage, Chiba 263-8522, Japan, and Phase Science, Diversity and Fractal Science, Graduate School of Nature Science and Technology, Chiba University, 1-33 Yayoi, Inage, Chiba 263-8522, Japan

Received: October 29, 1998; In Final Form: January 20, 1999

The X-ray diffraction (XRD) of C_2H_5OH molecules confined in slit-shaped graphitic micropores of activated carbon fibers having different pore widths was measured at 303 K. The effect of the pore width in the range 0.7−1.1 nm on the molecular assembly structure of C_2H_5OH in the micropores was examined. The XRD patterns were analyzed by use of the electron radial distribution function (ERDF) analysis. The densities of C_2H_5OH molecular assemblies in micropores were determined by C_2H_5OH adsorption at 303 K and N_2 adsorption at 77 K. The density of C_2H_5OH molecular assemblies in the 0.9 and 1.1 nm pores was close to the solid density of C_2H_5OH. The ERDFs showed that the first and second nearest-neighbor peaks shift to a shorter distance with a decrease of the pore width while their peak heights increase. These changes of the ERDFs coincided very well with the adsorbed density of C_2H_5OH, indicating that the serious confinement by the micropores gives rise to the solidlike ordering even at 303 K.

Introduction

In micropores the interaction potentials of a gas molecule with the pore walls overlap to give a deep potential well. Molecules tend to be adsorbed in the deep potential well.[1,2] The classical Gurvitch rule[1] guarantees the liquidlike structure formation of the adsorbed molecules in micropores. Furthermore, molecules adsorbed in the slit-shaped micropores are exposed to an asymmetric molecular field. That is, we can control the structure of the liquidlike molecular assembly of adsorbed molecules with micropores having an anisotropic molecular potential. Elucidation of the structure of the molecular assembly of adsorbed molecules in micropores should be helpful to understand the liquid structure. In particular, the effect of the pore width on the molecular assembly structure is important because the molecular potential well is governed by the pore width.

The authors have studied the structures of molecules confined in graphitic micropores for various molecules such as CCl_4,[3] N_2,[4] O_2,[5] NO,[6] SO_2,[7] He,[8] and H_2O.[9,10] CCl_4 molecules are nonpolar and roughly spherical and form a specific assembly structure of the low-temperature phase of bulk CCl_4 in micropores of a definite pore width at 303 K. H_2O molecules interact strongly with each other to produce a solidlike structure even at 303 K. The confined water does not freeze even at 143 K because the confined water is solidlike.[11] This ordered H_2O assembly can entrap methane molecules at 303 K even below 101 kPa.[12] Thus, micropores can be applied to control the intermolecular interaction.

A C_2H_5OH molecule has both polar and nonpolar sites. The relationship between the amphiphilicity and the assembly structure in micropores is quite important to understand the intermolecular interaction in the dense state. Also, C_2H_5OH has often been helpful to understand the special nature of liquid water in comparison with an organic solvent.[13]

This paper describes the orientational structure of the molecular assembly of C_2H_5OH in graphitic slit-shaped micropores using in situ X-ray diffraction experiments.

Experimental Section

Microporous Carbon Samples. Two kinds of pitch-based activated carbon fibers (ACFs) (P5 and P20) and the KOH-activated carbon (Max-31) were used. The micropore structures were determined by high-resolution N_2 adsorption isotherms at 77 K using a gravimetric method. The micropore structural parameters were obtained from high-resolution α_s-plot analysis for the N_2 adsorption isotherm in a way similar to those of preceding papers.[14,15]

C_2H_5OH Adsorption. The adsorption isotherm of C_2H_5OH on samples was gravimetrically measured at 303 K. The sample was preevacuated at 10 mPa and 383 K for 2 h.

In Situ X-ray Diffraction. The X-ray diffraction of C_2H_5-OH adsorbed in micropores of carbon samples was measured at 303 K by the transmission method using an angle-dispersive diffractometer (MXP3 system, MAC Science) in the scattering parameter $s(=4\pi\sin\theta/\lambda)$ range 3.1−125 nm^{-1}. The monochromatic Mo Kα ($\lambda = 7.093 \times 10^{-2}$ nm) at 50 kV and 30 mA was used for the diffraction measurement. We used an in situ X-ray diffraction chamber with Mylar film windows, which was reported in the previous paper.[3] The ground ACF samples were used for the X-ray diffraction measurement.

Results and Discussion

Density of C_2H_5OH Confined in Micropores. The N_2 adsorption isotherm of P5 was of type I. The N_2 adsorption isotherms of P20 and Max-31 had a linear adsorption increase until $P/P_0 = 0.4$ after an uptake in the low-pressure region. The adsorption data from $P/P_0 = 10^{-6}$ were used for determi-

[†] Physical Chemistry, Material Science.
[‡] Phase Science, Diversity and Fractal Science.

10.1021/jp984261v CCC: $18.00
Published on Web 03/03/1999

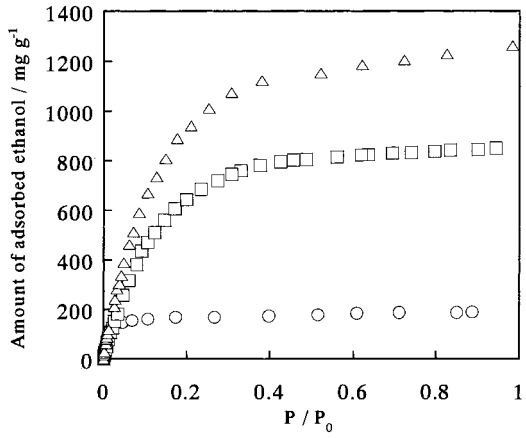

Figure 1. Adsorption isotherms of C_2H_5OH on carbon samples at 303 K: (○) P5; (□) P20; (△) Max-31.

TABLE 1: Micropore Volume W_0^N, Total Surface Area a_α, External Surface Area a_{ext}, and Average Pore Width w

	W_0^N/mL g^{-1}	a_α/m^2 g^{-1}	a_{ext}/m^2 g^{-1}	w/nm
P5	0.26	790	10	0.66
P20	0.79	1430	25	1.13
Max-31	1.11	2130	50	1.06

nation of the micropore structures with the subtracting pore effect (SPE) method for the high-resolution α_s-plot.[14,15] The features of the α_s-plot were similar to that published in an earlier paper.[12] The micropore volume W_0^N, total surface area a_α, external surface area a_{ext}, and the average pore width w are collected in Table 1. W_0^N, a_α, and a_{ext} can be determined from α_s-plots. The pore width w of slit-shaped micropores can be evaluated from both the surface area and pore volume using the simple geometrical relation

$$w = \frac{2W_0^N}{a_\alpha - a_{ext}} \tag{1}$$

Here, w is not the internuclear distance H between micropore walls. It means the width of the slit space available for adsorption. w can be approximated by $H - \sigma_c$, where σ_c is the Lennard-Jones size parameter of a carbon atom.

The adsorption isotherms of C_2H_5OH on carbon samples at 303 K were shown in Figure 1. All isotherms are of type I, being analogous to the N_2 adsorption isotherms. Hence, C_2H_5-OH molecules are adsorbed by the micropore filling mechanism. Figure 2 shows the Dubinin−Radushkevich (DR) plots; the DR equation is given in eq 2.

$$\ln W = \ln W_0 + \left(\frac{A}{\beta E_0}\right)^2; \quad A = RT\ln(P_0/P) \tag{2}$$

Here, W and W_0 are the amount of adsorption at P/P_0 and the pore volume, respectively. A is the adsorption potential, β and E_0 are the affinity coefficient and characteristic adsorption energy. Furthermore, βE_0 provides the isosteric heat of adsorption at fractional filling ϕ of e^{-1} with eq 3.

$$\beta E_0 + \Delta H_v = q_{st,\phi=1/e} \tag{3}$$

Here, ΔH_v is the enthalpy of vaporization. All DR plots are linear in the higher P_0/P region. The DR plot of P5 bends at $P_0/P = 44.6$ and becomes constant above $P_0/P = 44.6$. This indicates that these are small micropores in which N_2 can enter but C_2H_5OH cannot. On the other hand, the DR plots of P20

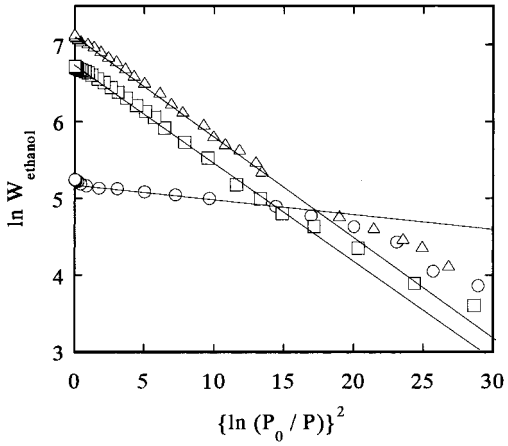

Figure 2. DR plots of C_2H_5OH adsorption isotherms at 303 K: (○) P5; (□) P20; (△) Max-31.

TABLE 2: Micropore Volume W_0^E, Isosteric Heat of Adsorption $q_{st,\phi=1/e}$, and Adsorbed Density ρ_a^E for Ethanol

	W_0^E/mL g^{-1}	$q_{st,\phi=1/e}$/kJ mol^{-1}	ρ_a^E/g cm^{-3}
P5	0.23	57.4	0.7
P20	1.06	45.6	1.1
Max-31	1.66	45.5	1.2

and Max-31 bend upward at $P_0/P = 63.0$ because of the different processes of micropore filling.

The micropore volume W_0^E determined from C_2H_5OH adsorption, $q_{st,\phi=1/e}$ and the adsorbed density ρ_a^E from C_2H_5OH adsorption are summarized in Table 2. ρ_a^E is the density of C_2H_5-OH adsorbed in micropores at the saturated vapor pressure and 303 K. Here, we used the liquid density of C_2H_5OH at 303 K for evaluation of W_0^E values. ρ_a^E was obtained from the adsorbed amount of C_2H_5OH in mg/g per W_0^N micropore volume determined by N_2 adsorption. The adsorbed density data suggest that the confined C_2H_5OH in P20 and Max-31 forms a denser structure than the bulk liquid at 303 K while the adsorbed C_2H_5-OH on P5 is sparse compared to the bulk liquid state. The densities of C_2H_5OH on P20 and Max-31 are very close to the bulk solid density of 1.025 g/cm^3 at 87 K,[16] which is far from the bulk liquid density of 0.7868 g/cm^3 at 303 K.

This adsorbed density indicates the presence of the serious restriction for packing of C_2H_5OH molecules in narrower micropores. Also, the $q_{st,\phi=1/e}$ value is larger than the isosteric heat of adsorption on graphite in the literature[17] by 7 kJ/mol for P20 and Max-31 and 19 kJ/mol for P5. The greater $q_{st,\phi=1/e}$ value supports a greater molecule−pore wall interaction. In particular, the predominant overlapping of the molecule−pore wall interactions should give rise to the greatest $q_{st,\phi=1/e}$ for P5.

X-ray Diffraction Patterns of Adsorbed C_2H_5OH Molecules. Figure 3 shows X-ray diffraction patterns of adsorbed C_2H_5OH, C_2H_5OH-adsorbed Max-31 and pure Max-31 at 303 K. The X-ray diffraction pattern of Max-31 has no (002) reflection near $s = 16$ nm^{-1}. However, the diffraction pattern of the C_2H_5OH-adsorbed Max-31 has a broad peak due to the adsorbed C_2H_5OH at $s = 15$ nm^{-1}. The difference of diffraction intensities between the C_2H_5OH-adsorbed Max-31 and Max-31 itself is assigned to the adsorbed C_2H_5OH molecular assemblies themselves with the assumption that the interference between adsorbed molecules and carbon walls is not predominant. Here, the small-angle X-ray scattering of Max-31 is greater than that of the C_2H_5OH-adsorbed sample because of the greater electron density difference between the carbon wall and the pore space; this small angle region was not used for further analysis because of the difficult correction. The X-ray diffraction of

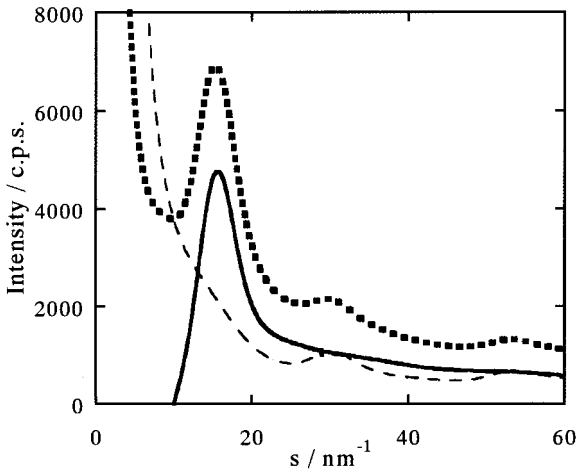

Figure 3. X-ray scattering intensities of Max-31 with adsorbed C_2H_5OH at 303 K: (dashed line) Max-31 itself; (dotted line) C_2H_5OH-adsorbed Max-31; (solid line) adsorbed C_2H_5OH.

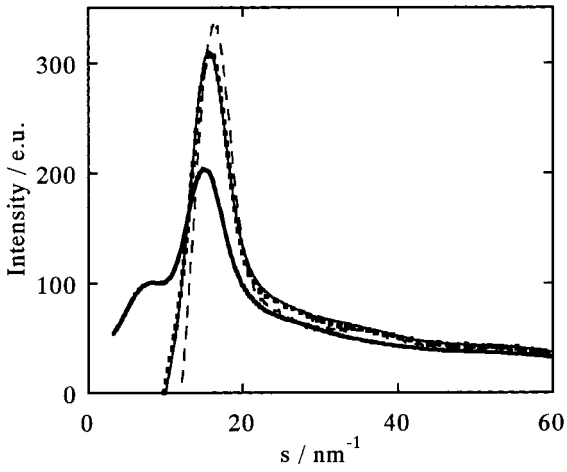

Figure 5. Corrected X-ray scattering intensities of C_2H_5OH adsorbed in carbon micropores: (dashed line) P5; (dotted line) P20; (fine solid line) Max-31; (bold solid line) pure liquid C_2H_5OH.

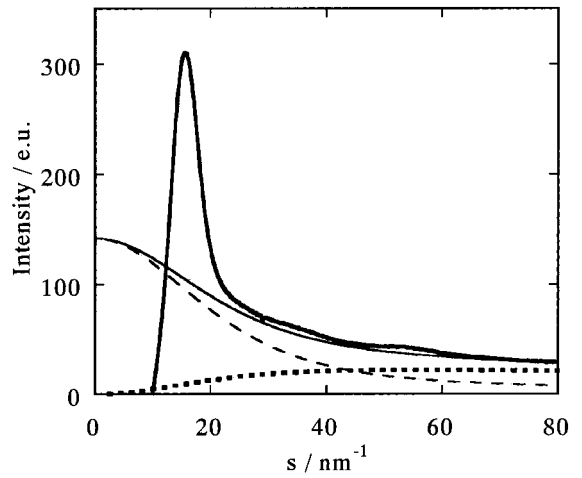

Figure 4. Corrected X-ray scattering intensities of C_2H_5OH on Max-31: (dashed line) coherent scattering intensity; (dotted line) incoherent scattering intensity; (fine solid line) sum of coherent and incoherent scattering intensities; (bold solid line) scattering intensity of adsorbed C_2H_5OH.

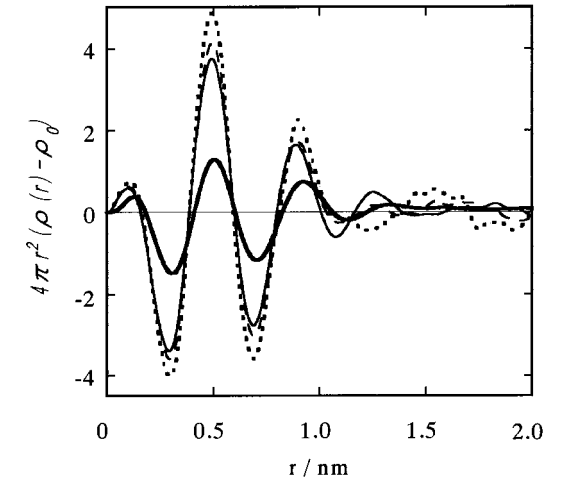

Figure 6. ERDFs of C_2H_5OH adsorbed in micropores of P20 as a function of the fractional filling ϕ at 303 K: (dotted line) $\phi = 0.27$; (dashed line) $\phi = 0.73$; (fine solid line) $\phi = 1$; (bold solid line) pure liquid C_2H_5OH.

adsorbed C_2H_5OH molecular assembly consists of coherent and incoherent X-ray scattering. Here, we removed the incoherent scattering by using literature values[18] that are multiplied by a function depending on the experimental condition of the monochromator. On the other hand, the coherent scattering was fitted to the self-scattering factor[18] at large s regions to normalize coherent scattering to the electron units, as shown in Figure 4.

Figure 5 shows the corrected X-ray diffraction patterns of C_2H_5OH adsorbed on carbon samples and for bulk liquid C_2H_5OH at 303 K. The slight difference is observed in the s range $10-30$ nm^{-1}. However, this broad diffraction pattern cannot provide the detailed structure of adsorbed C_2H_5OH. Therefore, we calculated the structure function of C_2H_5OH adsorbed in micropores of carbon samples. The structure function was Fourier transformed into the electron radial distribution function (ERDF).

Effect of Pore Width on Electron Radial Distribution Function of C_2H_5OH. Figure 6 shows the ERDFs of C_2H_5OH in micropores of P20 at different P/P_0. The ERDFs of liquid C_2H_5OH is also shown for comparison. The intensity of the peak of adsorbed C_2H_5OH at short range is higher than that of bulk liquid. The intensity of the peak in the short range for $\phi = 0.27$ is the greatest. The adsorbed C_2H_5OH has greater amplitudes than bulk liquid in the range $0.3-1.2$ nm. The first and second nearest peaks at 0.5 and 0.9 nm shift to a shorter distance compared with those of the bulk liquid. A periodic structure above 1.5 nm is observed for the adsorbed C_2H_5OH. This long-range ordering suggests that adsorbed C_2H_5OH molecules form highly ordered structures. However, the incomplete removal of the scattering between adsorbed molecules and pore walls may contribute to the long periodical structure to some extent. The higher peak and the peak shift suggest an immobile state of the adsorbed molecule and thereby that C_2H_5OH molecules adsorbed in micropores of P20 should have an ordered structure of less mobility.

Figure 7 shows ERDFs of C_2H_5OH adsorbed on three kinds of carbons at $P/P_0 = 1$ and 303 K. The amplitudes of ERDFs of confined C_2H_5OH are greater than those of the bulk liquid C_2H_5OH. The peak positions of the confined C_2H_5OH shift from those of the bulk liquid. The ERDFs of confined C_2H_5OH depend on the pore width. We calculated the radial distribution of the crystalline C_2H_5OH using the crystallographic data[16] and atomic scattering factors of carbon and oxygen atoms. As the crystalline structure gives a discontinuous distribution of the neighbor atoms, it is shown by vertical bars for which height is proportional to the coordination number. However, this calculated distribution is different from the average density. Hence,

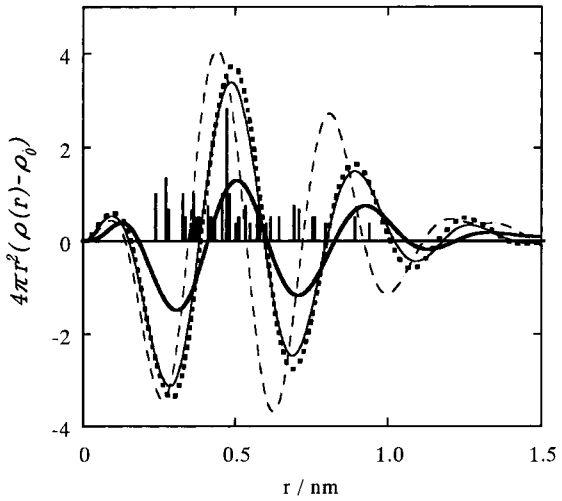

Figure 7. ERDFs of C_2H_5OH adsorbed in carbon micropores of three samples at $P/P_0 = 1$, 303 K: (dashed line) P5; (dotted line) P20; (fine solid line) Max-31; (bold solid line) pure liquid C_2H_5OH; (solid bars) positions and intensities for crystalline C_2H_5OH.

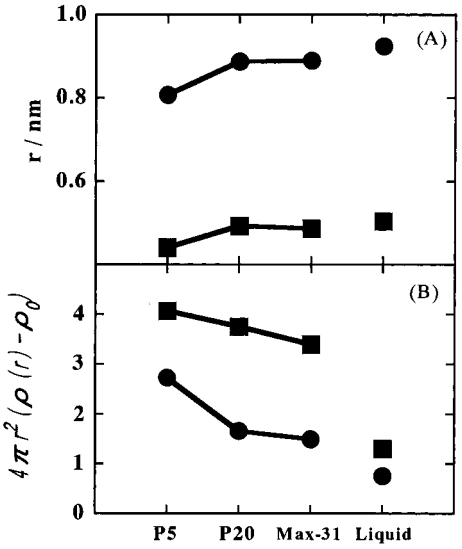

Figure 8. Changes in the position (A) and intensity (B) of the peaks of the first and second nearest neighbors: (■) first nearest neighbors; (●) second nearest neighbors.

we will use this calculated distribution for a qualitative structure determination of the confined C_2H_5OH. Especially, the peak positions of adsorbed C_2H_5OH at $r = 0.49$ nm for P20 and Max-31 are close to the peak position of the crystalline state at $r = 0.47$ nm. These results indicate that a solidlike structure is formed at short distances. On the other hand, the peak of adsorbed C_2H_5OH at $r = 0.44$ nm for P5 suggests the strong confinement of C_2H_5OH molecules in the narrower space and that these do not form the ordinary solid structure because of the serious confinement. Figure 8 shows the changes in the peak position (A) and peak intensity (B) of the first and second nearest neighbors with the pore width. The peak position increases with the pore width, approaching that of bulk liquid. On the other hand, the peak intensity decreases with the pore width. These tendencies hold for the peaks of both the first and second nearest neighbors. Both changes indicate that C_2H_5OH molecules should be confined strongly in narrower micropores.

Ordered Molecular Assembly Structure of Confined C_2H_5OH. The adsorbed density of C_2H_5OH molecules in larger micropores is not close to that of bulk liquid but to that of bulk solid. Also, the ERDF features strongly support the ordered structure formation. The C_2H_5OH molecule has CH_3 and OH groups that are hydrophobic and hydrophilic, respectively. The C_2H_5OH molecules should be associated with each other using hydrophobic and hydrophilic pairs. Jönsson examined the crystal structure of C_2H_5OH and showed that C_2H_5OH molecules are joined by two kinds of hydrogen bonds to form infinite zigzag chains.[16] Morishige et al. showed that C_2H_5OH molecules adsorbed on the graphite surface have a hydrogen-bonded specific structure at low temperature.[19] Thus, the hydrogen bonding plays an important role in the structure of C_2H_5OH molecular assemblies. The stabilization by the hydrogen bonding is more than 20 kJ/mol.[20] In the case of the ordered structure of C_2H_5OH molecules in micropores, the hydrogen bonds should play an essential role. We must take into account the adsorbed density, the crystal structure, and the possible hydrogen bonds for the ordered structure of C_2H_5OH molecules in micropores.

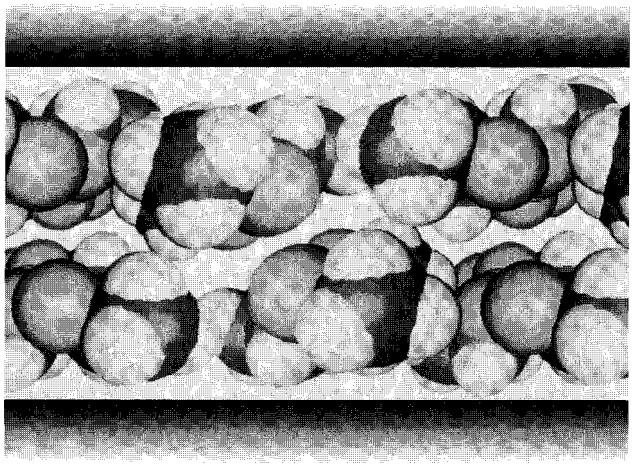

Figure 9. Model of adsorbed C_2H_5OH in P20 and Max-31.

Figure 9 shows the model of adsorbed C_2H_5OH in P20 and Max-31. The model structure for P20 and Max-31 was constructed from the crystal structure of the bulk solid C_2H_5-OH. This model is consistent with the observed ERDF and the density of C_2H_5OH adsorbed in micropores of P20 and Max-31. In contrast, micropores of P5 are too small to form the same structure as shown in Figure 9. We could construct an adsorbed model having the same molecular arrangement observed on the graphite surface at low temperature,[19] agreeing with the observed adsorbed density.

So far, we cannot determine precisely the atomic positions. In situ X-ray diffraction analysis and adsorption isotherm studies showed clearly that C_2H_5OH molecules in the hydrophobic nanospace form a solidlike ordered structure even at 303 K.

Acknowledgment. This work was funded by Japan Interaction in Science and Technology Forum and by the Grant-in-Aid for Scientific Research on Priority Areas No. 288 "Carbon Alloys" from the Japanese Government.

References and Notes

(1) Gregg, S. J.; Sing, K. S. W. *Adsorption, Surface Area and Porosity*; Academic Press: London, 1982.
(2) Kaneko, K. *J. Membr. Sci.* **1994**, *26*, 59.
(3) Iiyama, T.; Nishikawa, K.; Suzuki, T.; Otowa, T.; Hijiriyama, M.; Nojima, Y.; Kaneko, K. *J. Phys. Chem. B* **1997**, *101*, 3037.
(4) Kaneko, K.; Shimizu, K.; Suzuki, T. *J. Chem. Phys.* **1992**, *98*, 8705.
(5) Kanoh, H.; Kaneko, K. *J. Phys. Chem.* **1995**, *99*, 5746.
(6) Kaneko, K. *Collid Surf.* **1996**, *109*, 319.
(7) Wang, Z.-M.; Kaneko, K. *J. Phys. Chem.* **1995**, *99*, 155.
(8) Setoyama, N.; Kaneko, K.; Rodriguez-Reinoso, F. *J. Phys. Chem.* **1996**, *100*, 10331.

(9) Iiyama, T.; Nishikawa, K.; Otowa, T.; Kaneko, K. *J. Phys. Chem.* **1995**, *99*, 10075.
(10) Iiyama, T.; Nishikawa, K.; Suzuki, T.; Kaneko, K. *Chem. Phys. Lett.* **1997**, *274*, 152.
(11) Watanabe, A. *Chem. Phys. Lett.*, to be submitted.
(12) Miyawaki, J.; Kanda, T.; Suzuki, T.; Okui, T.; Maeda, Y.; Kaneko, K. *J. Phys. Chem. B* **1998**, *102*, 2187.
(13) Lamanna, R.; Cannistraro, S. *Chem. Phys.* **1996**, *213*, 95.
(14) Kaneko, K.; Ishii, C. *Colloids Surf.* **1992**, *67*, 203.
(15) Setoyama, N.; Suzuki, T.; Kaneko, K. *Carbon* **1998**, *36*, 1459.
(16) Jönsson, P.-G. *Acta Crystallogr. B* **1976**, *32*, 232.
(17) Kowalczyk, H.; Rychlicki, G.; Terzyk, A. P. *Pol. J. Chem.* **1993**, *67*, 2019.
(18) MacGillavry, C. H. *International Tables for X-ray Crystallography*; Kluwer Academic Publishers: Dordrecht, 1989; Vol. IV.
(19) Morishige, K. *J. Chem. Phys.* **1992**, *97*, 2084.
(20) Kolbe, A. *Z. Phys. Chem. (Leipzig)* **1972**, *250*, 183.